BEST AVAILABLE IMAGES

Defective images within this document are accurate representations of the original documents submitted by the applicant.

Defects in the images may include (but are not limited to):

- BLACK BORDERS
- TEXT CUT OFF AT TOP, BOTTOM OR SIDES
- FADED TEXT
- ILLEGIBLE TEXT
- SKEWED/SLANTED IMAGES
- COLORED PHOTOS
- BLACK OR VERY BLACK AND WHITE DARK PHOTOS
- GRAY SCALE DOCUMENTS

IMAGES ARE BEST AVAILABLE COPY.

As rescanning documents *will not* correct images, please do not report the images to the Image Problem Mailbox.

THE JOURNAL OF BIOLOGICAL CHEMISTRY

Vol. 278, No. 45, Issue of November 7, pp. 44886–44893, 2003
Printed in U.S.A.

Crystal Structures of Epothilone D-bound, Epothilone B-bound, and Substrate-free Forms of Cytochrome P450epoK*

Received for publication, July 25, 2003, and in revised form, August 15, 2003
Published, JBC Papers in Press, August 21, 2003, DOI 10.1074/jbc.M308115200

Shingo Nagano‡§, Huiying Li‡§, Hideaki Shimizu‡§¶, Clinton Nishida‖, Hiroshi Ogura‖, Paul R. Ortiz de Montellano‖, and Thomas L. Poulos‡§‡‡§§**

*From the ‡Department of Molecular Biology & Biochemistry, **Department of Physiology & Biophysics, ‡‡Department of Chemistry and the §Program in Macromolecular Structure, University of California, Irvine, Irvine, California 92697-3900 and the ‖Department of Pharmaceutical Chemistry, University of California, San Francisco, San Francisco, California 94143-2280*

Epothilones are potential anticancer drugs that stabilize microtubules by binding to tubulin in a manner similar to paclitaxel. Cytochrome P450epoK (P450epoK), a heme containing monooxygenase involved in epothilone biosynthesis in the myxobacterium *Sorangium cellulosum*, catalyzes the epoxidation of epothilones C and D into epothilones A and B, respectively. The 2.10-, 1.93-, and 2.65-Å crystal structures reported here for the epothilone D-bound, epothilone B-bound, and substrate-free forms, respectively, are the first crystal structures of an epothilone-binding protein. Although the substrate for P450epoK is the largest of a P450 whose x-ray structure is known, the structural changes along with substrate binding or product release are very minor and the overall fold is similar to other P450s. The epothilones are positioned with the macrolide ring roughly perpendicular to the heme plane and I helix, and the thiazole moiety provides key interactions that very likely are critical in determining substrate specificity. Interestingly, there are strong parallels between the epothilone/P450epoK and paclitaxel/tubulin interactions. Based on structural similarities, a plausible epothilone tubulin-binding mode is proposed.

Since the discovery of paclitaxel (an active ingredient of Taxol®) from *Taxus brevifolia* (1) and its clinical success as an anti-cancer drug, there have been extensive efforts to find compounds with similar action. Those efforts resulted in the identification of three other classes of compounds from natural sources: epothilones, produced by the cellulose-degrading myxobacterium *Sorangium cellulosum* (2), the marine sponge-derived discodermolide (3, 4), and the coral-derived eleutherobins (5)/sarcodictyins (6) (Fig. 1). All three classes, like paclitaxel, bind to and stabilize microtubules leading to mitotic arrest of the cycle at G_2-M phase and subsequently induction of cell death in several cell lines (7, 8). Epothilones, however, offer some advantages, because they are effective against P-glycoprotein-expressing multidrug-resistant cell lines, are active in a cell line with paclitaxel resistance (7), and the water solubility of epothilones is significantly greater than that of paclitaxel. Another advantage is that epothilones can be produced in large quantities using a heterologous expression system (9).

One step in the biosynthesis of epothilones involves a C12-C13 epoxidation (Fig. 1*a*) by a cytochrome P450, P450epoK (9). Cytochrome P450s (P450s)[1] are heme-containing monooxygenases best known for their role in drug detoxification (10). However, P450s also are involved in steroid hormone biosynthesis (11) as well as the biosynthesis of important macrolide antibiotics like erythromycin (12) and rapamycin (13). To date, there is no known protein structure complexed with an epothilone. In addition, epothilone represents the largest substrate of a P450 where the crystal structure of the enzyme-substrate complex is known and thus provides important insights in understanding how P450 architecture adapts to the requirements of substrate binding. Here we present the crystal structures of the oxidized P450epoK in substrate-free, epothilone D-bound, and epothilone B-bound forms at 2.65-, 2.10-, and 1.93-Å resolution, respectively.

EXPERIMENTAL PROCEDURES

Protein Purification and Crystallization—P450epoK was overexpressed in *Escherichia coli* and purified as will be described elsewhere.[2] Single crystals of all forms of P450epoK reported here were obtained by the vapor-diffusion method using the sitting-drop technique. P450epoK crystals were obtained within a few days after microseeding. Crystals of the imidazole-bound form for multiple wavelength anomalous diffraction (MAD) phasing were grown at 23 °C in 100 mM imidazole, pH 6.5/50 mM NaCl/16% polyethylene glycol 5000 monomethyl ether. The initial droplets contained 1 μl of protein solution at a concentration of 40 mg/ml and 1 μl of precipitant solution and were equilibrated against a reservoir containing 500 μl of precipitant solution. Crystals of the substrate-free form were also obtained by vapor-diffusion method at 23 °C from 18% polyethylene glycol 5000 monomethyl ether/0.1 M Li_2SO_4/0.1 M MES, pH 6.5. Initial protein concentration was 20 mg/ml. Crystals of epothilone-bound P450epoK were grown at 23 °C from 11% of polyethylene glycol 550 monomethyl ether/0.05 M glycine, pH 8.4, in the presence of a saturated amount of epothilone B or D. The microseeding method was also used for these crystal growths. The single crystal was carefully transferred to cryobuffer containing glycerol with the glycerol concentration brought up to 20% in four steps.

Data Collection and Processing—With the exception of MAD data, x-ray diffraction data were collected at the Advanced Light Source, Lawrence Berkeley Laboratory, beam line 8.2.2 with an Area Detector System Corporation Quantum 315 charge-coupled device detector at cryogenic temperature. MAD data sets of imidazole-bound P450epoK were collected at the Stanford Synchrotron Radiation Laboratory beam

* This work was supported by National Institutes of Health Grants GM33688 (to T. L. P.) and GM25515 (to P. R. O. d. M.), by biostar00-10100 (to P. R. O. d. M.), and by a postdoctoral fellowship from Japan Society for the Promotion of Science (to S. N.). The costs of publication of this article were defrayed in part by the payment of page charges. This article must therefore be hereby marked "*advertisement*" in accordance with 18 U.S.C. Section 1734 solely to indicate this fact.

¶ Present address: Molecular Neuropathology Group, RIKEN Brain Science Inst., 2-1 Hirosawa, Wako-shi, Saitama 351-0198, Japan.

§§ To whom correspondence should be addressed. Tel.: 949-824-7020; Fax: 949-824-3280; E-mail: poulos@uci.edu.

[1] The abbreviations used are: P450, cytochrome P450; MAD, multiple wavelength anomalous diffraction; MES, 4-morpholineethanesulfonic acid; 6-DEB, 6-deoxyerythronolide B; r.m.s., root mean square.

[2] C. Nishida, H. Ogura, and P. R. Ortiz de Montellano, unpublished data.

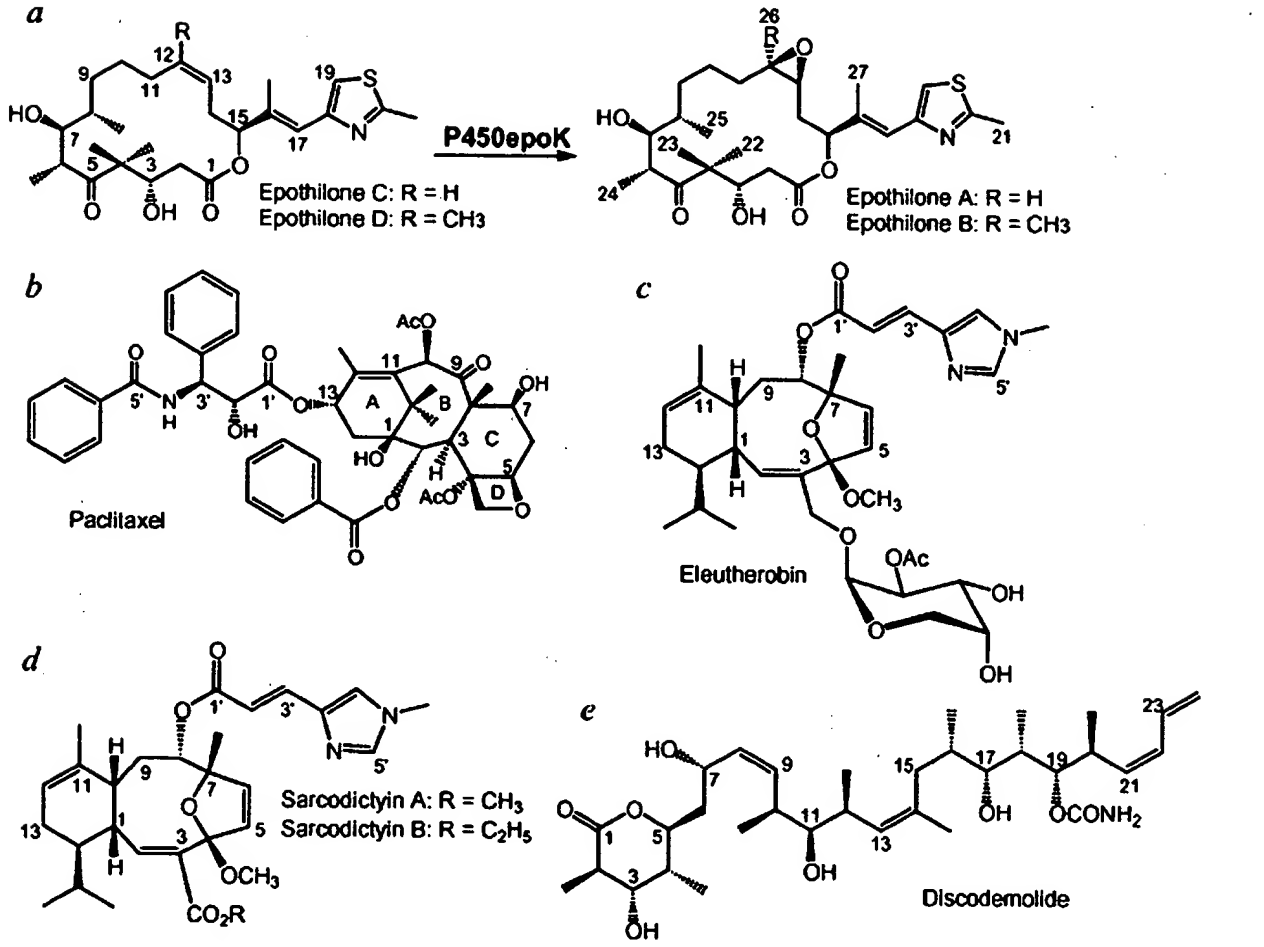

FIG. 1. **Tubulin-binding anti-cancer drugs.** *a*, structure of epothilones and epoxidation reaction catalyzed by P450epoK. Epothilones D and B have higher tubulin polymerization activity and cytotoxicity than epothilones C and A, respectively (8, 45). *b*, paclitaxel. Taxane skeleton is composed of rings A–D. *c*, eleutherobin; *d*, sarcodictyin; *e*, discodemolide.

TABLE I
Data collection and refinement statistics for substrate-free, epothilone D-bound, and epothilone B-bound forms

Data set	Substrate-free	Epothilone D-bound	Epothilone B-bound
Unit cell (Å)	$a = b = 61.52$; $c = 256.73$	$a = b = 60.43$; $c = 252.77$	$a = b = 61.52$; $c = 252.84$
Space group	$P4_322$	$P4_322$	$P4_322$
Resolution range (Å)	50–2.65	50–2.10	50–1.93
Reflections (observed/unique)	72,065/14,049	167,058/27,331	203,413/34,489
R_{merge} (overall/outer shell; %)	7.7/39.6	6.3/34.2	9.2/37.8
$\langle I/\sigma(I)\rangle$ (overall/outer shell)	19.5/2.7	33.9/3.7	25.9/2.4
Completeness (overall/outer shell; %)	91.7/94.9	96.2/95.4	91.0/72.4
R/R_{free} (%)	23.4/29.9	21.6/27.3	21.5/25.9
r.m.s.d. bond length (Å)	0.016	0.015	0.010
r.m.s.d. bond angle (degree)	1.56	1.50	1.25
Number of water molecules	103	200	266

line 1–5 with an Area Detector System Corporation Quantum-4R charge-coupled device detector. Three wavelengths around the iron edge, 1.738 Å (peak), 1.741 Å (inflection), and 1.653 Å (remote), were chosen. The inverse-beam data collection procedure was used to ensure good completeness and redundancy for Bijvoet pairs. Data were processed and scaled using HKL2000 (14). Crystallographic statistics are given in Table I.

MAD Phasing—The iron position was located, and initial phases were refined with three-wavelength MAD data sets at 2.9 Å using SOLVE (15) enabling the location of several α-helices and bulky side chains. Solvent flattening and density modification using RESOLVE (16) resulted in a more clearly interpretable electron density map. Statistics for the MAD data sets are given in Table II.

Model Building, Refinement, and Cavity Volume Calculation—A polyalanine model of P450eryF was used as a reference for the initial electron density map fitting using the graphical model building program O (17). Model refinement was carried out with CNS (18) and REFMAC (19) using the maximum likelihood protocol. Cavity volumes for substrate-free P450epoK and P450cam were calculated by the use of the program VOIDOO (20). All figures were prepared using MOLSCRIPT (21), RASTER3D (22), or PYMOL (www.pymol.org).

RESULTS AND DISCUSSION

Comparison with Other P450s—To accommodate the bulky substrate, epothilone, P450epoK has a large substrate-binding cavity of 1060 Å^3 in volume. Despite the presence of the very large substrate binding site, the overall structure of P450epoK and its outer dimensions are similar to that of P450cam (23) whose substrate binding cavity is only 240 Å^3 in volume. Like other P450s, P450epoK exhibits the typical triangular prism-shaped P450 fold (Fig. 2*a*) with a side 60 Å long and 30 Å thick and the heme prosthetic group embedded between the I and L

TABLE II
Statistics of imidazole-bound form for MAD phasing

	λ_1	λ_2	λ_3
Wavelength (Å)	1.7383	1.7409	1.6531
Resolution range (Å)	50–2.9	50–2.9	50–2.9
Observations (observed/unique)	85,431/16,746	86,845/16,656	82,898/16,460
Completeness (overall/outer shell; %)	83.6/54.6	83.5/55.6	82.5/53.4
R_{merge} (overall/outer shell; %)	4.2/17.8	4.0/18.5	3.4/15.6
$\langle I/\sigma(I)\rangle$ (overall/outer shell)	34.9/3.9	34.3/3.7	36.6/4.5
Figure of merit		0.51	

helices. In addition, the substrate binding cavity is surrounded mainly by the heme and the I and F helices (Fig. 2*b*). Although the folds are the same, P450epoK and P450cam differ in the location of several helices (Fig. 3). The significant differences, which are important for substrate binding (24, 25), include the B′, F, and G helices (Figs. 3 and 4*a*). The B′ helix of P450cam is important for substrate binding, especially via an H-bond between Tyr^{96} and the camphor carbonyl oxygen atom. In P450epoK the B′ helix region is composed of two helices, B′1 and B′2. Both helices are farther from the active site than the B′ helix in P450cam to accommodate the larger substrate. The B′2 helix is especially important, because residues from this helix help to form part of the substrate binding pocket. On the other hand, the F helix, which forms the roof over the substrate, is even closer to the heme than that of P450cam. The closer approach of the F helix to the active is possible, because the C-terminal end of the F helix has smaller side chains on the side facing the heme: Gly^{176} and Ala^{180}, which correspond to Thr^{181} and Thr^{185} of P450cam, respectively. This close approach of the F helix to the substrate or product enables the carbonyl O atom of Ala^{180} in the F helix to accept an H-bond from the substrate/product C3 OH group, which will be considered in more detail below.

As in other P450s, the I helix experiences a kink near a conserved Thr residue, Thr^{258} in P450epoK, that is important to the oxygen activation machinery (26, 27). Another conserved structural element in P450s is the Cys thiolate heme ligand and its immediate surroundings. P450epoK is no exception with Cys^{365} near the N-terminal end of the L helix coordinating the heme iron (Fig. 2*b*). Also similar to other P450s are the H-bond and ionic interactions between the heme propionates and His and Arg residues (Arg^{107}, His^{103}, and Arg^{307} in P450epoK).

Of the known P450 structures, the closest homologue to P450epoK at 30% identity and 48% similarity is P450eryF (28), which also utilizes a polyketide, 6-deoxyerythronolide B (6-DEB), as a substrate. As seen for the substrate bound to P450eryF (28), epothilones D and B are oriented roughly perpendicular to the heme plane and I helix (Figs. 2*b* and 5). P450eryF has a long loop preceding the B′ helix, which might provide flexibility required to accommodate the large 14-member ring of 6-DEB. However, this loop is much shorter in P450epoK despite the larger size of epothilone. The F helix of P450epoK (Cys^{168}-Leu^{183}), which forms the roof of the substrate binding site, exhibits a 4.7-Å r.m.s. difference in backbone compared with P450eryF (Glu166-Val176), and is positioned closer to the heme for protein-substrate interactions. The G helix (Glu194-Asn219) exhibits a 4.8-Å r.m.s. difference in backbone, and its N-terminal position is located farther from the heme than in P450eryF (Arg^{181}-Glu^{206}). The relocation of these helices results in a P450epoK F/G loop that is 5 residues longer than the corresponding loop in P450eryF. The longer F/G loop could provide additional flexibility for substrate entry.

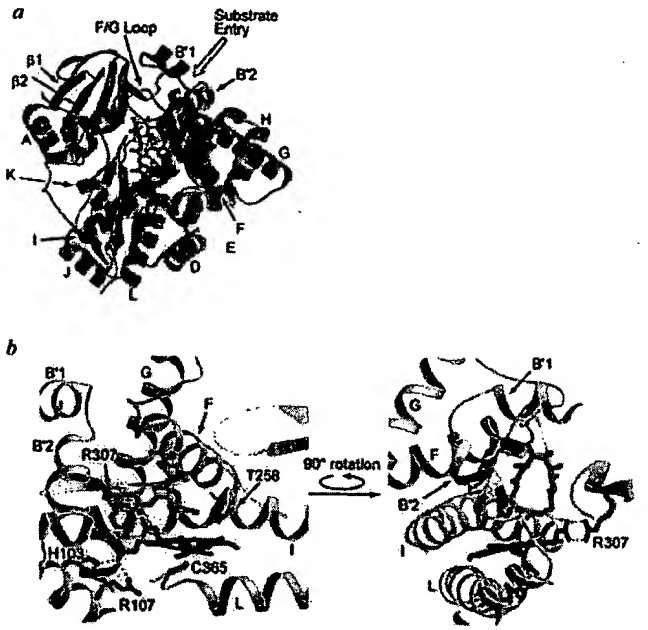

FIG. 2. **Overall and active site structure of oxidized P450epoK complexed with epothilone D.** The heme prosthetic group and epothilone D are shown as *red* and *cyan sticks*, respectively. *a*, overall structure. Helices and β-structures are shown in *green* and *orange*, respectively. The plausible substrate entry channel is indicated. Secondary structures were assigned by using PROCHECK (46). *b*, active site structure of epothilone D-bound P450epoK. Thr^{258}, which is important to oxygen activation, the proximal heme ligand, Cys^{365}, and the residues involved in heme anchoring are displayed as *stick models*.

In addition to the size of the macrolide ring, another important difference between P450epoK and P450eryF is that in P450epoK the macrolide ring of the substrate is rotated about 90° relative to 6-DEB (Fig. 4*b*). This is necessary to accommodate the thiazole ring. The only other orientation of epothilone that would position the C12-C13 double bond for proper epoxidation would have the thiazole ring pointing toward the I helix. Because the I helix is one of the most conserved regions in P450 and is critical for oxygen activation (26, 27, 29), large variations in the I helix cannot be tolerated. Therefore, the thiazole ring must point toward the B′2 helix thus requiring a reorientation of the macrolide ring relative to P450eryF. In P450epoK this region is farther from the active site and provides side chains such as Phe^{96} that specifically interact with the thiazole ring.

Heme Coordination—Normally substrate-free oxidized P450s are low spin with a water molecule coordinated to the sixth coordination position. Upon substrate binding, this ligand is displaced giving a penta-coordinate high spin heme (30, 31). P450epoK is somewhat different, because the epothilone B and D complexes give a low spin species (spectra not shown) like substrate-bound P450BSβ, which has a water molecule at the sixth coordination site (32). Consistent with a low spin heme, the structure reveals that a water molecule, which is H-bonded to the epothilone B epoxide O atom (Fig. 5*b*), is coordinated to the heme iron. The substrate-free and epothilone D-bound structures are low spin and expected to be hexa-coordinate. Although there is some electron density at the sixth coordination site, the limited resolution of the substrate-free data, 2.65 Å, precludes a clear identification of a single water molecule coordinated to the heme iron.

Conformational Changes upon Epothilone Binding—Until now P450cam (23, 33), P450BM-3 (34, 35), and P450 2C5 (36, 37) were the only P450s where both the substrate-free and

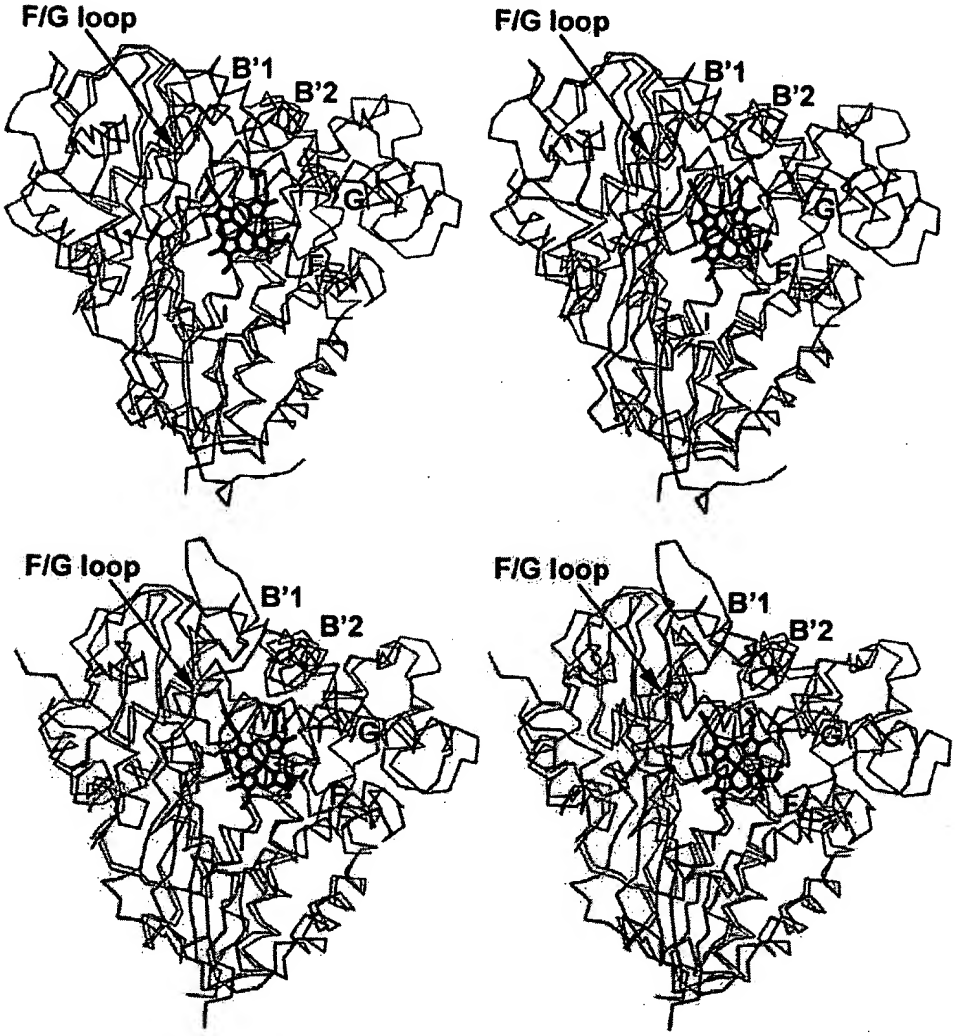

FIG. 3. **Stereo diagram of superimposed P450s.** *Top panel*, P450epok (*red*) on P450cam (*green*). *Bottom panel*, P450epok (*red*) on P450eryF (*green*). The models were superimposed by overlaying the heme groups. Key helical regions and the F/G loop are labeled.

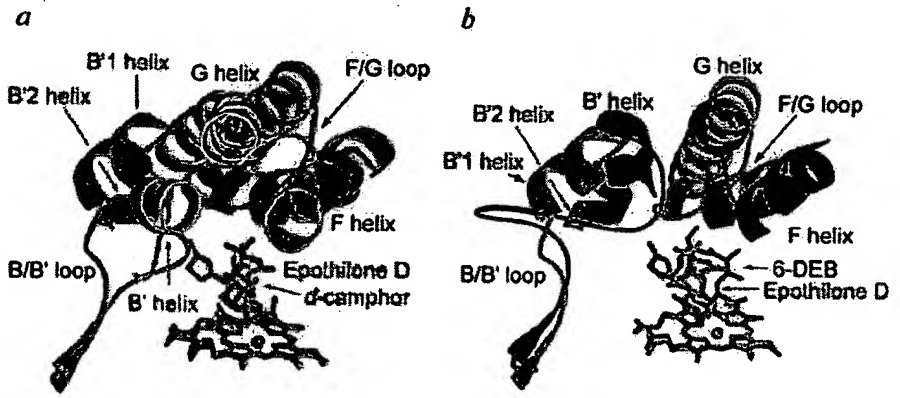

FIG. 4. **Superimposed structures of F, G, and B' helices and connecting loops.** *a*, P450epoK (*green*) and P450cam (*cyan*). *b*, P450epoK (*green*) and P450eryF (*red*). The substrates (epothilone D for P450epoK; *d*-camphor for P450cam; 6-DEB for P450eryF) and heme are shown as *stick models*.

-bound crystal structures are known, whereas P450cam was the only structure with product bound (38). P450epoK represents the second example where all three structures are known. In P450cam there is very little difference in structures between the three forms, whereas with P450BM-3, there are large changes between the substrate-free and -bound structures primarily due to motions of the F and G helices and the F/G loop (34), whereas with P450 2C5 similar but smaller changes are observed (37). Large changes in these regions also have been observed upon ligand binding for a thermophilic P450, CYP119 (39). Given that epothilone is the largest substrate of a P450 with known structure, we anticipated some significant changes in structure upon substrate binding. However, the differences between the substrate-bound and -free P450epoK structures are small and are confined to the F/G loop and B'1 helix regions (Fig. 6, *a* and *b*) generally thought to provide the entry point for substrates in P450s (24). The B'1 helix moves closer toward and the F/G loop moves away from the active site to optimize interactions with the substrate. These differences are similar to what was observed in the

P450BM-3 substrate-bound (34) and -free (35) forms except the changes are much smaller in P450epoK. It appears that the plausible substrate access channel, indicated in Fig. 2*a*, is similar to what has been proposed for P450BM-3 and P450cam. However, P450epoK must be able to adopt an even more open conformation to allow substrate entry and product release. That the substrate-free P450epoK crystallized in the nearly closed form is very likely due to crystal packing forces favoring the substrate-bound closed conformation as opposed to the postulated open conformation. With the substrate-free P450BM-3 just the opposite occurred: crystal packing favored the open form (35).

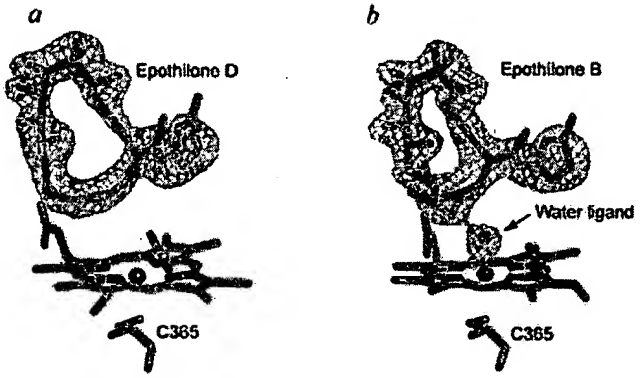

FIG. 5. **Simulated annealing $F_o - F_c$ omit maps.** The final models are overlaid on the map contoured at the 3.0-σ level. Carbon atoms of epothilone are shown in *cyan* except for the C12-C13 double bond which is *yellow*. Protein and heme carbon atoms are *green*. Nitrogen, oxygen, and sulfur atoms are shown in *blue*, *red*, and *orange*, respectively. *a*, epothilone D-bound form; *b*, epothilone B-bound form.

In addition to a small adjustment in the backbone, various side chains move to accommodate the substrate. Most notable is Arg^{71} in the loop between B and B'1 helix, the guanidium group of which moves about 4 Å closer to the active site (Fig. 6*c*). This movement enables Arg^{71} to hold two water molecules close to the substrate, especially the thiazole ring. In addition, the movement of Arg^{71} enables the thiazole ring to form a π-π stacking interaction with Phe^{96}, whose side chain provides a key substrate contact.

Epothilone/P450epoK Interactions—As found for P450eryF (28), there are a number of water molecules around epothilone that form H-bonding bridges between epothilone and protein atoms (Fig. 7). The H-bond network involves 6 residues for the epothilone D-bound form and 7 residues for the epothilone B-bound form, respectively. Most of the residues involved in these backbone H-bonds are small, such as Gly and Ala, which provide the required room for the large substrate. Arg^{71}, which, as already mentioned, moves into the active site upon epothi-

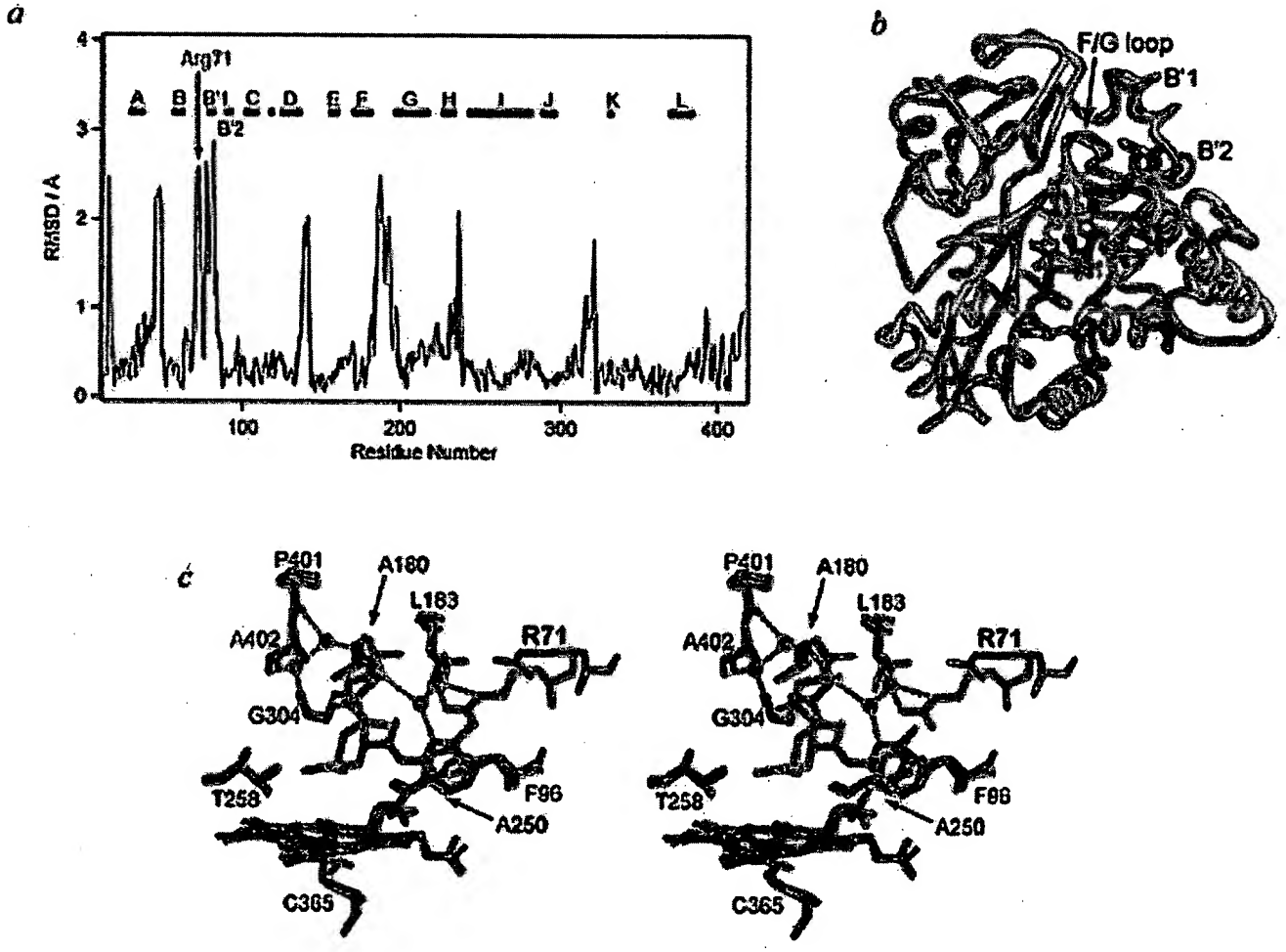

FIG. 6. **Structural changes upon epothilone D-binding.** *a*, r.m.s. deviation between substrate-free and epothilone D-bound P450epoK plotted against residue number with the helical regions indicated. The location of Arg^{71} is highlighted. *b*, superposition of Cα-traces of substrate-free (*gray*) and substrate-bound (*green*) P450epoK. The orientation is the same as in Fig. 2*a*. The heme and substrate are shown as *stick models*. *c*, stereo view showing conformational changes around the epothilone-binding site. The heme and amino acid residues, which are important for the epothilone binding and catalytic activity, are shown in *gray* for substrate-free and in *green* for epothilone D-bound forms. Epothilone D is shown as a *stick model* (carbon, *cyan*; nitrogen, *blue*; sulfur, *orange*; and oxygen, *red*).

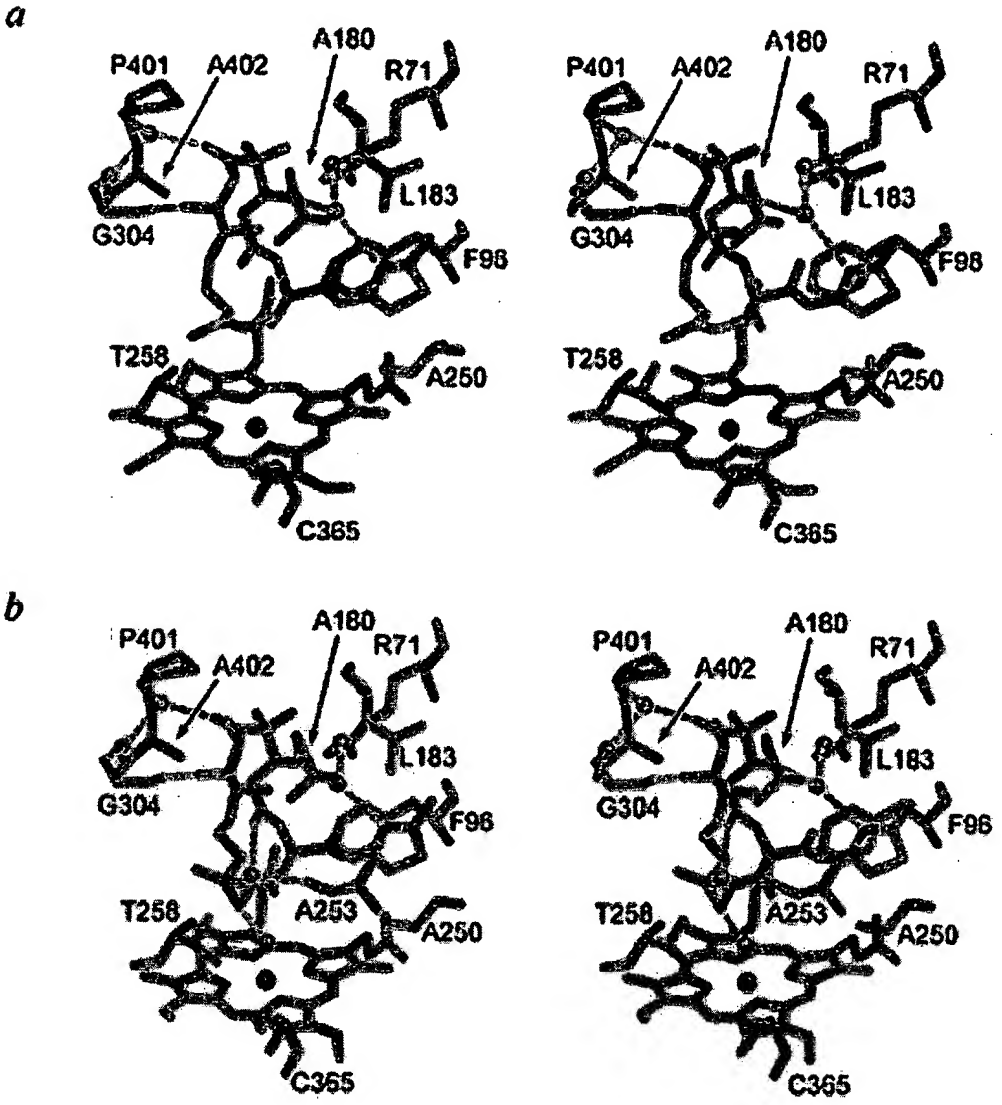

FIG. 7. **Stereo view showing substrate-binding site.** Atom colors are the same as in Fig. 4. H-bonds, which bridge between epothilone and protein atoms, are shown as *broken yellow lines*. *a*, epothilone D-bound form; *b*, epothilone B-bound form.

lone binding, is the only the side chain that forms part of the H-bond network with the substrate. Phe^{96}, which forms π-π stacking interactions with the thiazole ring and the guanidium group of Arg^{71}, is very likely a critical residue for epothilone specificity. In addition to H-bonding and aromatic interactions, Leu^{183} in the F helix and Ala^{250} in the I helix form non-bonded contacts with the substrate/product thiazole ring (Fig. 7).

Similar to other P450s, the carbons to be oxidized are close to the heme iron (Figs. 5*a* and 7*a*). In this case, the C12-C13 double bond reacts with the iron-linked oxygen atom to give an epoxide. The distances of C12-Fe and C13-Fe are 4.7 and 5.0 Å, respectively, which are comparable to the distance between the iron and the carbon atom to be hydroxylated in P450cam and P450eryF (4.2 and 4.7 Å, respectively). The substrate orientation is suitable for synchronous oxygen transfer from an Fe(IV)-O species.

The conformation of P450epoK-bound epothilones is somewhat different from the crystal structure of free epothilone (2). The thiazole side chain is perpendicular to the macrolide ring in P450epoK, whereas free epothilone has the thiazole moiety in-plane with the macrolide ring. However, the conformation of the macrolide ring predicted to bind to tubulin (31) is the same as that bound to P450epoK.

Implication for Tubulin/Epothilone Interactions—Both paclitaxel and epothilone bind to tubulin to stabilize microtubules, arresting cells in mitosis. Epothilones competitively inhibit the binding of paclitaxel to polymerized tubulin, suggesting that the two types of antitumor compounds share an overlapping binding site in tubulin (7, 8). Therefore, it is of interest to see if the binding of epothilones to P450epoK mimic to any degree the interactions found between paclitaxel and tubulin (40). As shown in Fig. 8, the C2-phenyl ring of paclitaxel is the structural homologue to the epothilone thiazole ring. Both form π-π stacking interactions with a neighboring aromatic ring (His^{229} of β-tubulin and Phe^{96} of P450epoK) in addition to other non-bonded contacts with aliphatic side chains (Leu^{217} of β-tubulin and Ala^{250} of P450epoK). The aromatic moiety of epothilone is critical, because its removal or direct attachment of the aromatic moiety to C15 results in the loss of tubulin binding and cytotoxic properties (41). Therefore, it is reasonable to expect that the thiazole ring of epothilone makes similar π-π stacking interaction when it binds to tubulin. Structure-activity relationship studies on epothilones have also shown that the location of the N atom in the aromatic ring is important for tubulin binding activity, because the 2-pyridyl- and 2-thiazyl-containing compounds exhibit properties comparable to the natural

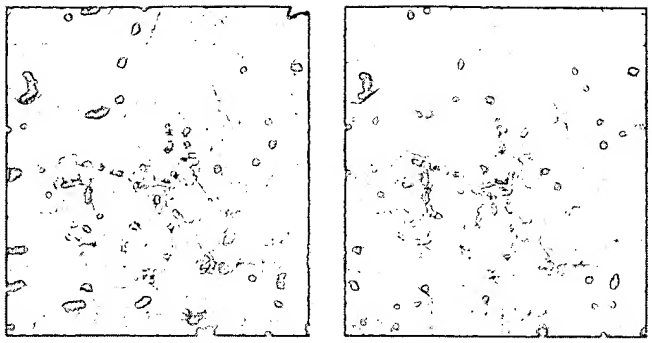

FIG. 8. **Electron crystallographic structure of paclitaxel bound to β-tubulin (40).** Paclitaxel and β-tubulin are shown as stick (*yellow*, carbon; *blue*, nitrogen; and *red*, oxygen) and surface models, respectively. *Orange surface* shows the position of Phe^{272}, which is replaced with Val in β-tubulin of paclitaxel-resistant cells (42). *Green surface* shows the position of Thr^{276} (*lower*) and Arg^{284} (*upper*), which are replaced with Ile and Gln, respectively, in β-tubulin of epothilone-resistant cells (43).

product, but 3-pyridyl and 5-thiazyl compounds were much less active (41). In the epothilone-bound P450epoK structures, the N atom of the thiazole ring H-bonds to water molecules, which interact with the enzyme and macrolide ring. Therefore, it is interesting to note that the predicted site for the thiazole ring interaction in tubulin places the ring close to potential H-bonding groups such as Asp^{226}, peptide groups, or a water molecule.

A greater challenge is predicting the macrolide ring binding site on tubulin, although there is a molecular modeling studies in epothilone/tubulin interaction (42). Drug sensitivity data for several paclitaxel- and epothilone-resistant cell lines provide some additional clues. 1A9PTX10 cells derived from a human ovarian carcinoma cells shows paclitaxel resistance (42). These cells have the mutation F272V in β-tubulin, which would be expected to affect paclitaxel binding, because Phe^{272} is located near the taxane ring of paclitaxel (Fig. 8). On the other hand, it would be expected that epothilone is located farther away from this site, because these cells retained significant epothilone B sensitivity. Two other mutations, T276I and R284Q, impair epothilone sensitivity in 1A9/A8 and 1A9B10 cells, respectively (43), while exhibiting only a minor effect on paclitaxel sensitivity further indicating the taxane ring of paclitaxel and macrolide ring of epothilone bind differently. From these arguments, we propose that the macrolide ring of epothilone binds close to Thr^{276} and Arg^{284} while the thiazole ring is in the crevice between His^{229} and Leu^{217}. To locate the macrolide ring near Thr^{276} and Arg^{284}, the conformation of the macrolide ring must flip by about 90° relative to the thiazole ring observed in the P450epoK structure. Such an adaptation of epothilone to the putative binding site would be possible owing to flexibility of epothilone as indicated by the quite different conformations of free epothilone and epothilone bound to P450epoK.

Another class of tubulin-stabilizing anticancer drug, sarcodictyin and eleutherobin (Fig. 1, *c* and *d*), also have a five-membered aromatic group, methyl imidazole, attached to the main frame with the linker (-OCOCH=CH-), which is of similar length to the epothilone linker (-CH=C(CH_3)-). In addition, as found for epothilone, eleutherobin is a competitive inhibitor of the paclitaxel binding to tubulin (44). These common structural features of drugs, 5- or 6-member aromatic rings, together with the similar π-π stacking interactions for paclitaxel/tubulin and epothilone/P450epoK, suggest that these aromatic rings are indispensable for tubulin binding and/or stabilization of polymerized tubulin.

CONCLUSIONS

Although epothilone is the largest natural substrate for P450 with known structure, the overall fold of P450epoK is very similar to other P450s. Unexpectedly, the structures of the substrate/product-bound P450epoK are very similar to the substrate-free structure with no major changes in the substrate access channel. Because P450epoK must undergo a large open/close motion to allow substrate to enter, we attribute crystal packing forces as the reason substrate-free P450epoK crystallized in the closed form. The largest change observed is in Arg^{71}, which moves into the active site to help critical water molecules maintain H-bonds to the substrate/product. Similarities of how the thiazole ring of epothilone interacts in the P450epoK active site to how paclitaxel interacts with tubulin together with the mutant data suggest a possible binding mode for epothilone to tubulin.

Acknowledgments—We thank the staffs at the Stanford Synchrotron Radiation Laboratory and Advanced Light Source for their generous assistance with data collection.

REFERENCES

1. Wani, M. C., Taylor, H. L., Wall, M. E., Coggon, P., and McPhail, A. T. (1971) *J. Am. Chem. Soc.* **93,** 2325–2327
2. Höfle, G. H., Bedorf, N., Steinmetz, H., Schomburg, D., Gerth, K., and Reichenbach, H. (1996) *Angew. Chem. Int. Ed. Engl.* **35,** 1567–1569
3. Kowalski, R. J., Giannakakou, P., Gunasekera, S. P., Longley, R. E., Day, B. W., and Hamel, E. (1997) *Mol. Pharmacol.* **52,** 613–622
4. ter Haar, E., Kowalski, R. J., Hamel, E., Lin, C. M., Longley, R. E., Gunasekera, S. P., Rosenkranz, H. S., and Day, B. W. (1996) *Biochemistry* **35,** 243–250
5. Lindel, T., Jensen, P. R., Fenical, W., Long, B. H., Casazza, A. M., Carboni, J., and Fairchild, C. R. (1997) *J. Am. Chem. Soc.* **119,** 8744–8745
6. Dambrosio, M., Guerriero, A., and Pietra, F. (1987) *Helv. Chim. Acta* **70,** 2019–2027
7. Bollag, D. M., McQueney, P. A., Zhu, J., Hensens, O., Koupal, L., Liesch, J., Goetz, M., Lazarides, E., and Woods, C. M. (1995) *Cancer Res.* **55,** 2325–2333
8. Kowalski, R. J., Giannakakou, P., and Hamel, E. (1997) *J. Biol. Chem.* **272,** 2534–2541
9. Tang, L., Shah, S., Chung, L., Carney, J., Katz, L., Khosla, C., and Julien, B. (2000) *Science* **287,** 640–642
10. Ortiz de Montellano, P. R. (1997) *Cytochrome P450: Structure, Mechanism, and Biochemistry*, 2nd Ed., Plenum Press, New York
11. Kagawa, N., and Waterman, M. R. (1997) in *Cytochrome P450: Structure, Mechanism, and Biochemistry* (Ortiz de Montellano, P. R., ed) 2nd Ed., pp. 419–442, Plenum Press, New York
12. Andersen, J. F., and Hutchinson, C. R. (1992) *J. Bacteriol.* **174,** 725–735
13. Molnar, I., Aparicio, J. F., Haydock, S. F., Khaw, L. E., Schwecke, T., Konig, A., Staunton, J., and Leadlay, P. F. (1996) *Gene (Amst.)* **169,** 1–7
14. Otwinowski, Z., and Minor, W. (1997) *Methods Enzymol.* **276,** 307–326
15. Terwilliger, T. C., and Berendzen, J. (1999) *Acta Crystallogr. Sect. D Biol. Crystallogr.* **55,** 849–861
16. Terwilliger, T. C. (2000) *Acta Crystallogr. Sect. D Biol. Crystallogr.* **56,** 965–972
17. Jones, T. A., Zou, J. Y., Cowan, S. W., and Kjeldgaard, M. (1991) *Acta Crystallogr. Sect. A* **47,** 110–119
18. Brunger, A. T., Adams, P. D., Clore, G. M., DeLano, W. L., Gros, P., Grosse-Kunstleve, R. W., Jiang, J. S., Kuszewski, J., Nilges, M., Pannu, N. S., Read, R. J., Rice, L. M., Simonson, T., and Warren, G. L. (1998) *Acta Crystallogr. Sect. D Biol. Crystallogr.* **54,** 905–921
19. Murshudov, G. N., Vagin, A. A., Lebedev, A., Wilson, K. S., and Dodson, E. J. (1999) *Acta Crystallogr. Sect. D Biol. Crystallogr.* **55,** 247–255
20. Kleywegt, G. J., and Jones, T. A. (1994) *Acta Crystallogr. Sect. D Biol. Crystallogr.* **50,** 178–185
21. Kraulis, P. J. (1991) *J. Appl. Crystallogr.* **24,** 946–950
22. Merritt, E. A., and Murphy, M. E. P. (1994) *Acta Crystallogr. Sect. D Biol. Crystallogr.* **50,** 869–873
23. Poulos, T. L., Finzel, B. C., Gunsalus, I. C., Wagner, G. C., and Kraut, J. (1985) *J. Biol. Chem.* **260,** 16122–16130
24. Winn, P. J., Ludemann, S. K., Gauges, R., Lounnas, V., and Wade, R. C. (2002) *Proc. Natl. Acad. Sci. U. S. A.* **99,** 5361–5366
25. Gotoh, O. (1992) *J. Biol. Chem.* **267,** 83–90
26. Martinis, S. A., Atkins, W. M., Stayton, P. S., and Sligar, S. G. (1989) *J. Am. Chem. Soc.* **111,** 9252–9253
27. Imai, M., Shimada, H., Watanabe, Y., Matsushimahibiya, Y., Makino, R., Koga, H., Horiuchi, T., and Ishimura, Y. (1989) *Proc. Natl. Acad. Sci. U. S. A.* **86,** 7823–7827
28. Cupp-Vickery, J. R., and Poulos, T. L. (1995) *Nat. Struct. Biol.* **2,** 144–153
29. Gerber, N. C., and Sligar, S. G. (1994) *J. Biol. Chem.* **269,** 4260–4266
30. Tsai, R., Yu, C. A., Gunsalus, I. C., Peisach, J., Blumberg, W., Orme-Johnson, W. H., and Beinert, H. (1970) *Proc. Natl. Acad. Sci. U. S. A.* **66,** 1157–1163
31. Sligar, S. G. (1976) *Biochemistry* **15,** 5399–5406
32. Lee, D. S., Yamada, A., Sugimoto, H., Matsunaga, I., Ogura, H., Ichihara, K., Adachi, S., Park, S. Y., and Shiro, Y. (2003) *J. Biol. Chem.* **278,** 9761–9767
33. Poulos, T. L., Finzel, B. C., and Howard, A. J. (1986) *Biochemistry* **25,**

5314–5322
34. Li, H., and Poulos, T. L. (1997) *Nat. Struct. Biol.* **4**, 140–146
35. Ravichandran, K. G., Boddupalli, S. S., Hasermann, C. A., Peterson, J. A., and Deisenhofer, J. (1993) *Science* **261**, 731–736
36. Williams, P. A., Cosme, J., Sridhar, V., Johnson, E. F., and McRee, D. E. (2000) *Mol. Cell.* **5**, 121–131
37. Wester, M. R., Johnson, E. F., Marques-Soares, C., Dansette, P. M., Mansuy, D., and Stout, C. D. (2003) *Biochemistry* **42**, 6370–6379
38. Li, H. Y., Narasimhulu, S., Havran, L. M., Winkler, J. D., and Poulos, T. L. (1995) *J. Am. Chem. Soc.* **117**, 6297–6299
39. Yano, J. K., Koo, L. S., Schuller, D. J., Li, H., Ortiz de Montellano, P. R., and Poulos, T. L. (2000) *J. Biol. Chem.* **275**, 31086–31092
40. Löwe, J., Li, H., Downing, K. H., and Nogales, E. (2001) *J. Mol. Biol.* **313**, 1045–1057
41. Nicolaou, K. C., Roschangar, F., and Vourloumis, D. (1998) *Angew. Chem. Int. Ed. Engl.* **37**, 2014–2045
42. Giannakakou, P., Sackett, D. L., Kang, Y. K., Zhan, Z. R., Buters, J. T. M., Fojo, T., and Poruchynsky, M. S. (1997) *J. Biol. Chem.* **272**, 17118–17125
43. Giannakakou, P., Gussio, R., Nogales, E., Downing, K. H., Zaharevitz, D., Bollbuck, B., Poy, G., Sackett, D., Nicolaou, K. C., and Fojo, T. (2000) *Proc. Natl. Acad. Sci. U. S. A.* **97**, 2904–2909
44. Hamel, E., Sackett, D. L., Vourloumis, D., and Nicolaou, K. C. (1999) *Biochemistry* **38**, 5490–5498
45. Chou, T. C., Zhang, X. G., Balog, A., Su, D. S., Meng, D. F., Savin, K., Bertino, J. R., and Danishefsky, S. J. (1998) *Proc. Natl. Acad. Sci. U. S. A.* **95**, 9642–9647
46. Laskowski, R. A., Macarthur, M. W., Moss, D. S., and Thornton, J. M. (1993) *J. Appl. Crystallogr.* **26**, 283–291